

地球表層の水の量

(出典：ENCYCLOPEDIA of HYDROLOGY AND WATER RESORCES, 1998)

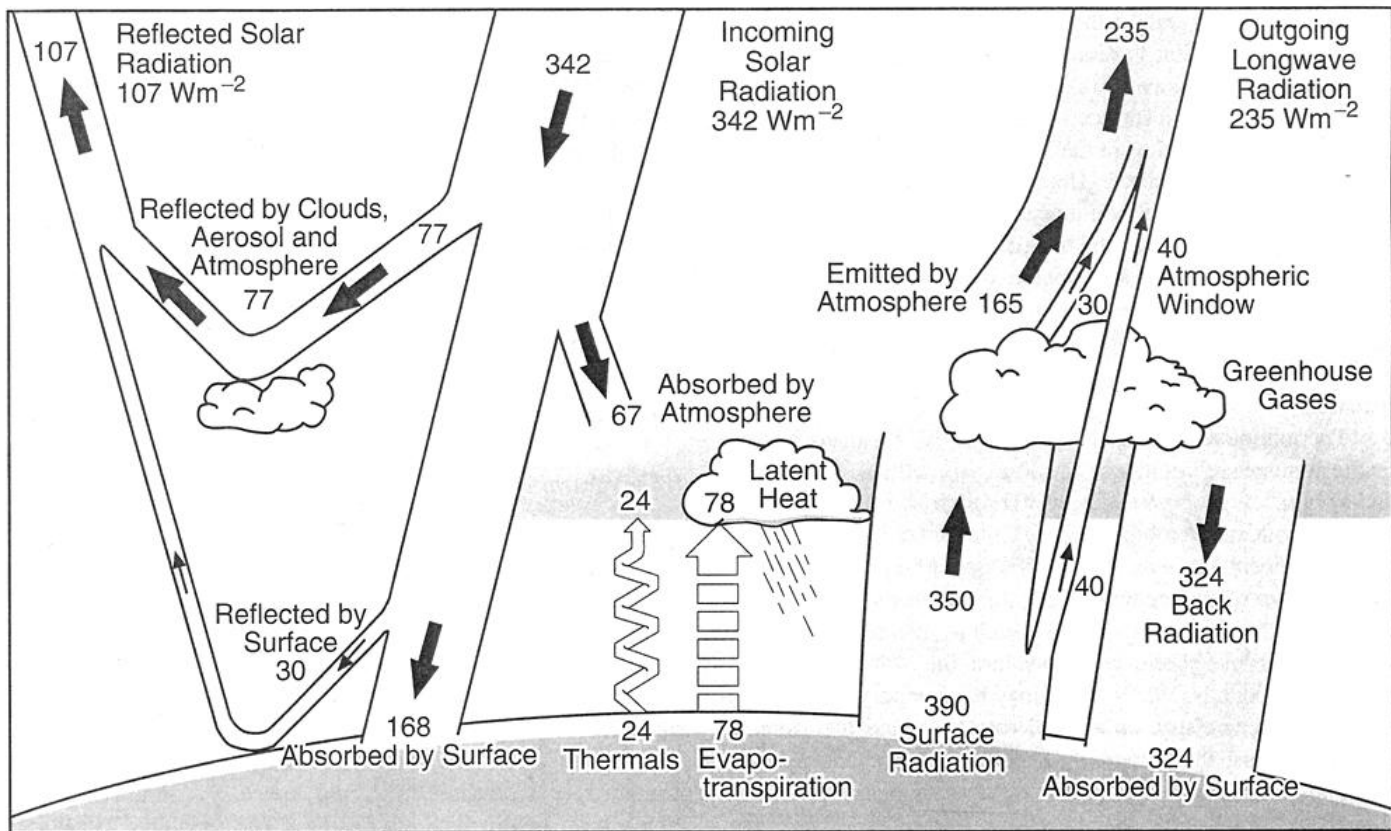


図3 地球大気のエネルギーバランス (IPCC第3次報告書より)

温暖化概論(水循環)

地球水循環研究センター
中村健治

Global warming

Clapeyron-Claucius's law \rightarrow 7 % each 1 degree Celcius.

Model: o. k.

Data: not clear

Complex, spatial/temporal variations

Difficult to get reliable results from data analyses

Local

Warming inversely correlate with precipitation.
However, some area, positively correlates.

Extremes affect long-term trends.

Frequency of El Nino, number of typhoons, Sahel drought, etc.

Global warming

Reduction of snow -- > reduction of snow on mountains

Aerosol effects

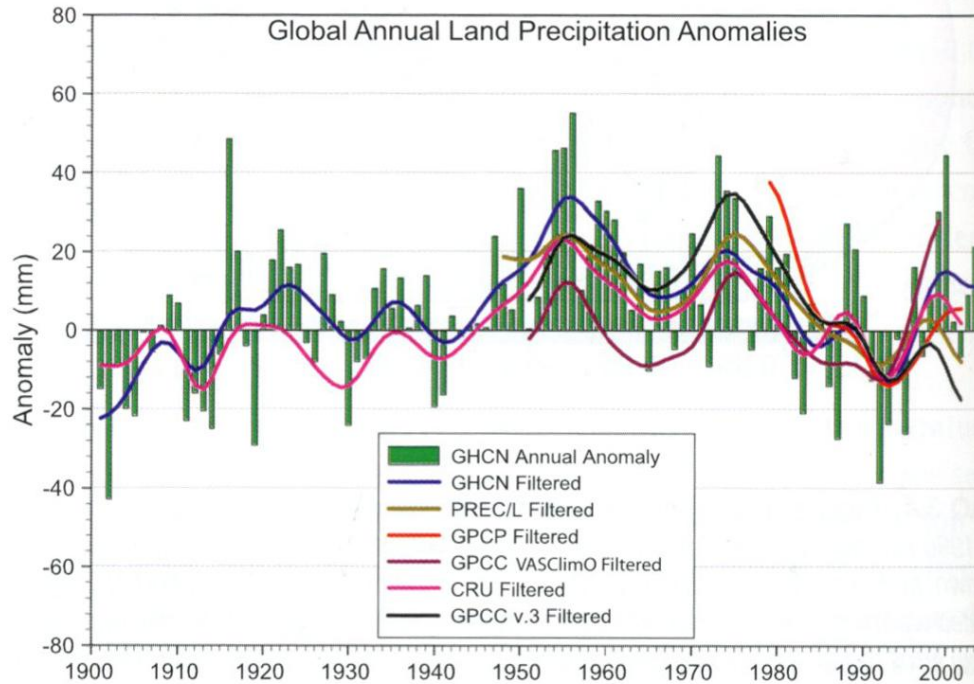


Figure 3.12. Time series for 1900 to 2005 of annual global land precipitation anomalies (mm) from GHCN with respect to the 1981 to 2000 base period. The smooth curves show decadal variations (see Appendix 3.A) for the GHCN (Peterson and Vose, 1997), PREC/L (Chen et al., 2002), GPCP (Adler et al., 2003), GPPC (Rudolf et al., 1994) and CRU (Mitchell and Jones, 2005) data sets.

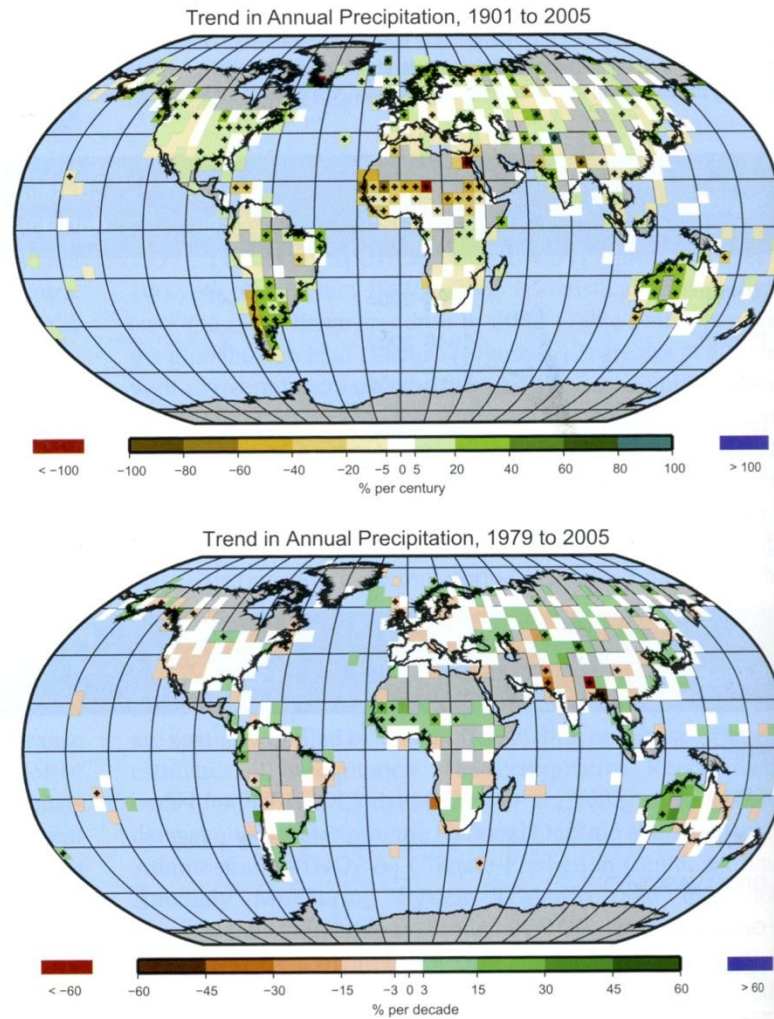
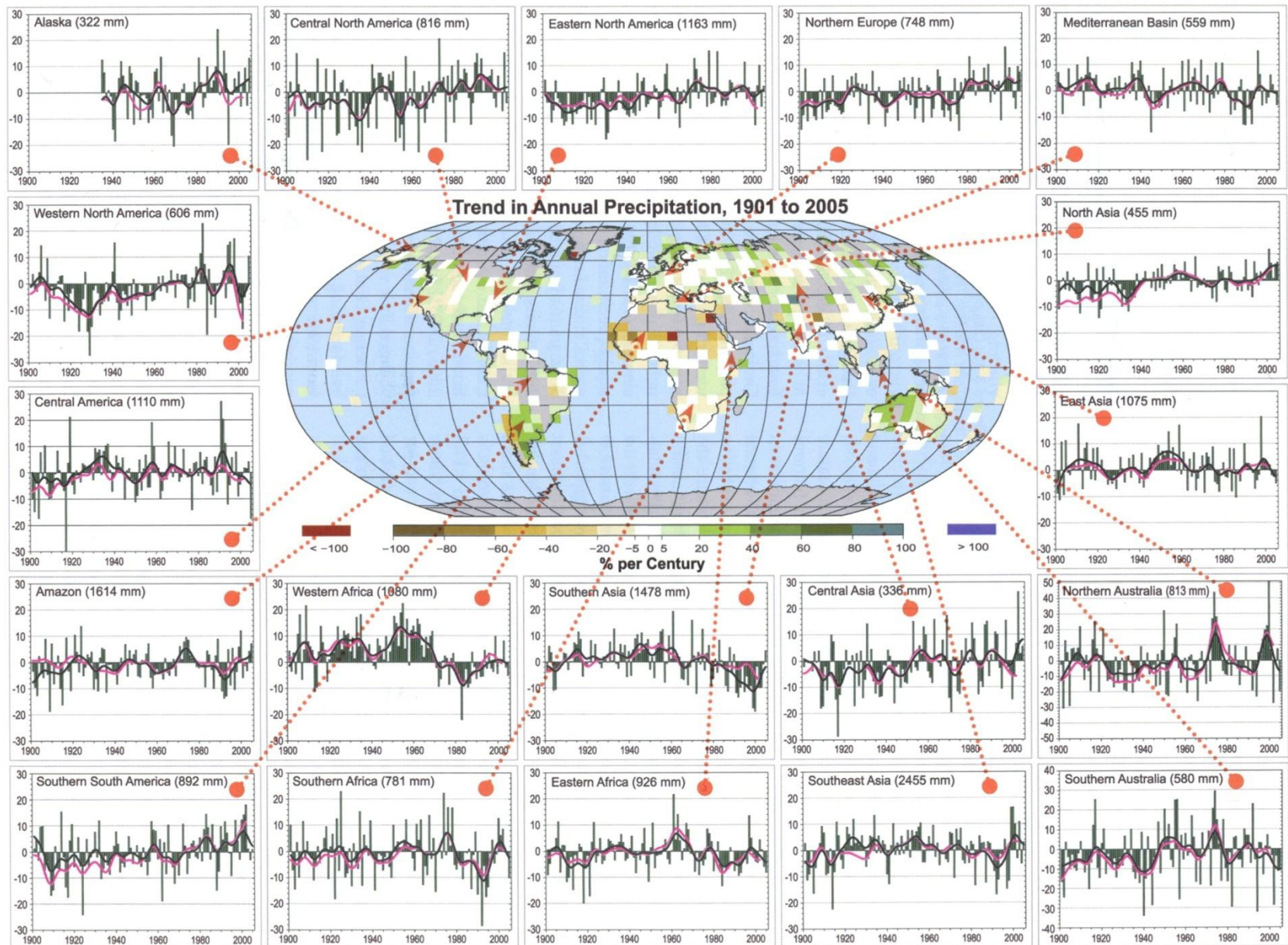
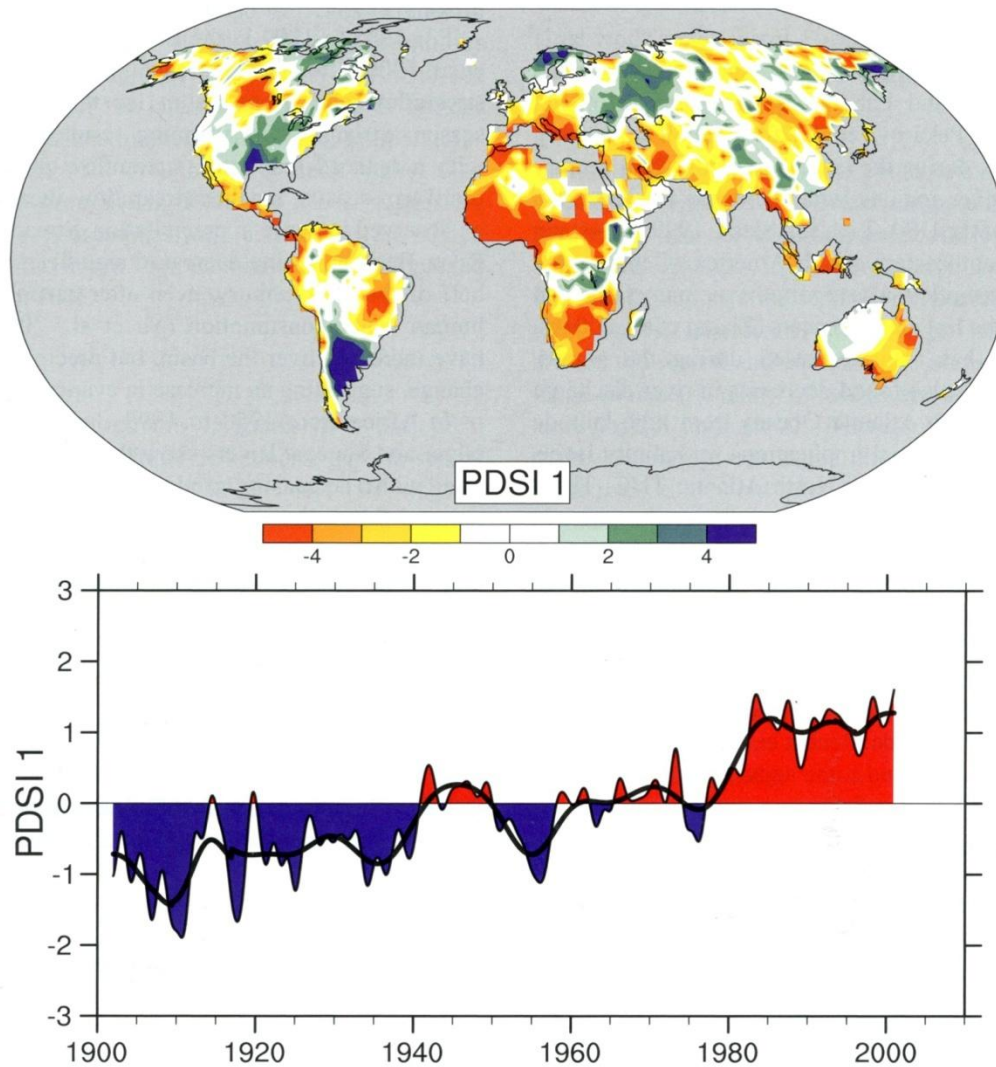


Figure 3.13. Trend of annual land precipitation amounts for 1901 to 2005 (top, % per century) and 1979 to 2005 (bottom, % per decade), using the GHCN precipitation data set from NCDC. The percentage is based on the means for the 1961 to 1990 period. Areas in grey have insufficient data to produce reliable trends. The minimum number of years required to calculate a trend value is 66 for 1901 to 2005 and 18 for 1979 to 2005. An annual value is complete for a given year if all 12 monthly percentage anomaly values are present. Note the different colour bars and units in each plot. Trends significant at the 5% level are indicated by black + marks.

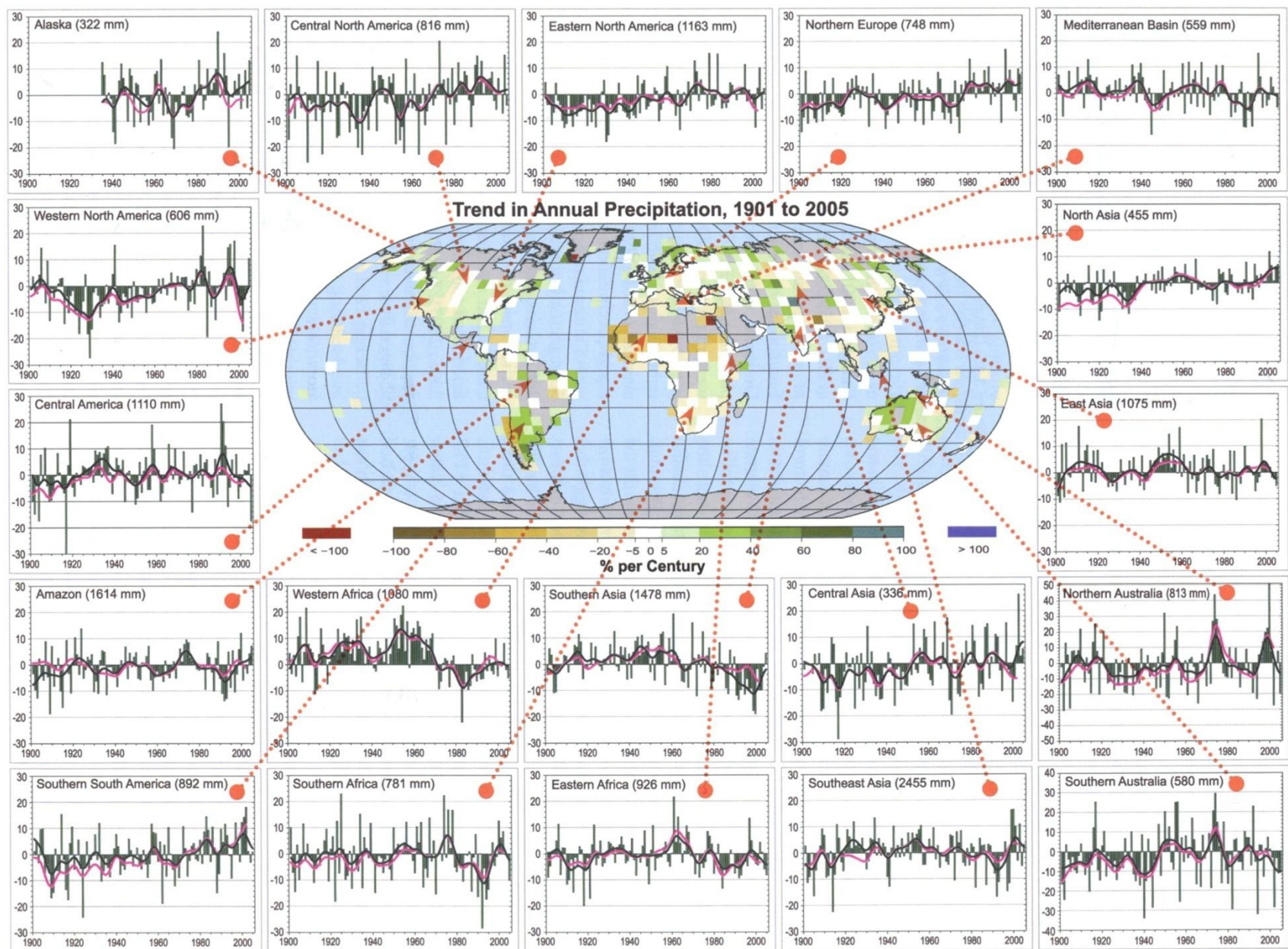
Figure 3.14. Precipitation for 1900 to 2005. The central map shows the annual mean trends (% per century). Areas in grey have insufficient data to produce reliable trends. The surrounding time series of annual precipitation displayed (% of mean, with the mean given at top for 1961 to 1990) are for the named regions as indicated by the red arrows. The GHCN precipitation from NCDC was used for the annual green bars and black for decadal variations (see Appendix 3.A), and for comparison the CRU decadal variations are in magenta. The range is +30 to -30% except for the two Australian panels. The regions are a subset of those defined in Table 11.1 (Section 11.1) and include: Central North America, Western North America, Alaska, Central America, Eastern North America, Mediterranean, Northern Europe, North Asia, East Asia, Central Asia, Southeast Asia, Southern Asia, Northern Australia, Southern Australia, Eastern Africa, Western Africa, Southern Africa, Southern South America, and the Amazon.





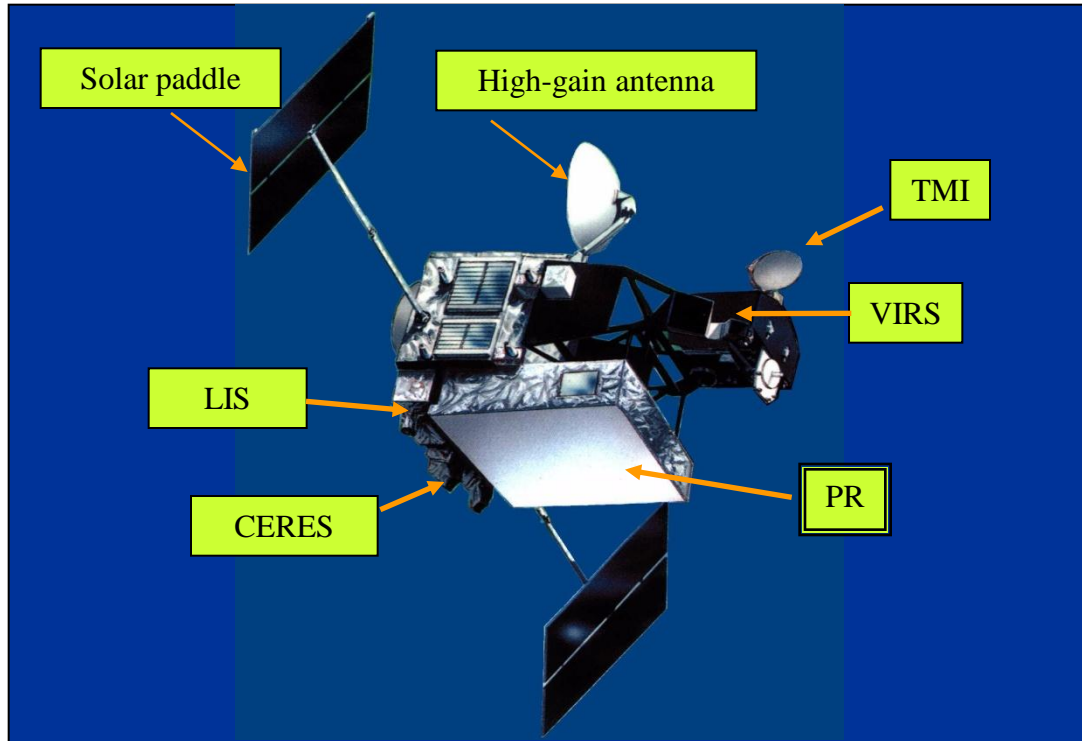
FAQ 3.2, Figure 1. The most important spatial pattern (top) of the monthly Palmer Drought Severity Index (PDSI) for 1900 to 2002. The PDSI is a prominent index of drought and measures the cumulative deficit (relative to local mean conditions) in surface land moisture by incorporating previous precipitation and estimates of moisture drawn into the atmosphere (based on atmospheric temperatures) into a hydrological accounting system. The lower panel shows how the sign and strength of this pattern has changed since 1900. Red and orange areas are drier (wetter) than average and blue and green areas are wetter (drier) than average when the values shown in the lower plot are positive (negative). The smooth black curve shows decadal variations. The time series approximately corresponds to a trend, and this pattern and its variations account for 67% of the linear trend of PDSI from 1900 to 2002 over the global land area. It therefore features widespread increasing African drought, especially in the Sahel, for instance. Note also the wetter areas, especially in eastern North and South America and northern Eurasia. Adapted from Dai et al. (2004b).

Figure 3.14. Precipitation for 1900 to 2005. The central map shows the annual mean trends (% per century). Areas in grey have insufficient data to produce reliable trends. The surrounding time series of annual precipitation displayed (% of mean, with the mean given at top for 1961 to 1990) are for the named regions as indicated by the red arrows. The GHCN precipitation from NCDC was used for the annual green bars and black for decadal variations (see Appendix 3.A), and for comparison the CRU decadal variations are in magenta. The range is +30 to -30% except for the two Australian panels. The regions are a subset of those defined in Table 11.1 (Section 11.1) and include: Central North America, Western North America, Alaska, Central America, Eastern North America, Mediterranean, Northern Europe, North Asia, East Asia, Central Asia, Southeast Asia, Southern Asia, Northern Australia, Southern Australia, Eastern Africa, Western Africa, Southern Africa, Southern South America, and the Amazon.





Tropical Rainfall Measuring Mission: TRMM



Observation of tropical rainfall (Driving engine of global atmosphere)

US-Japan joint mission (Japan: PR, Launch, US: Bus, 4 sensors, operation)

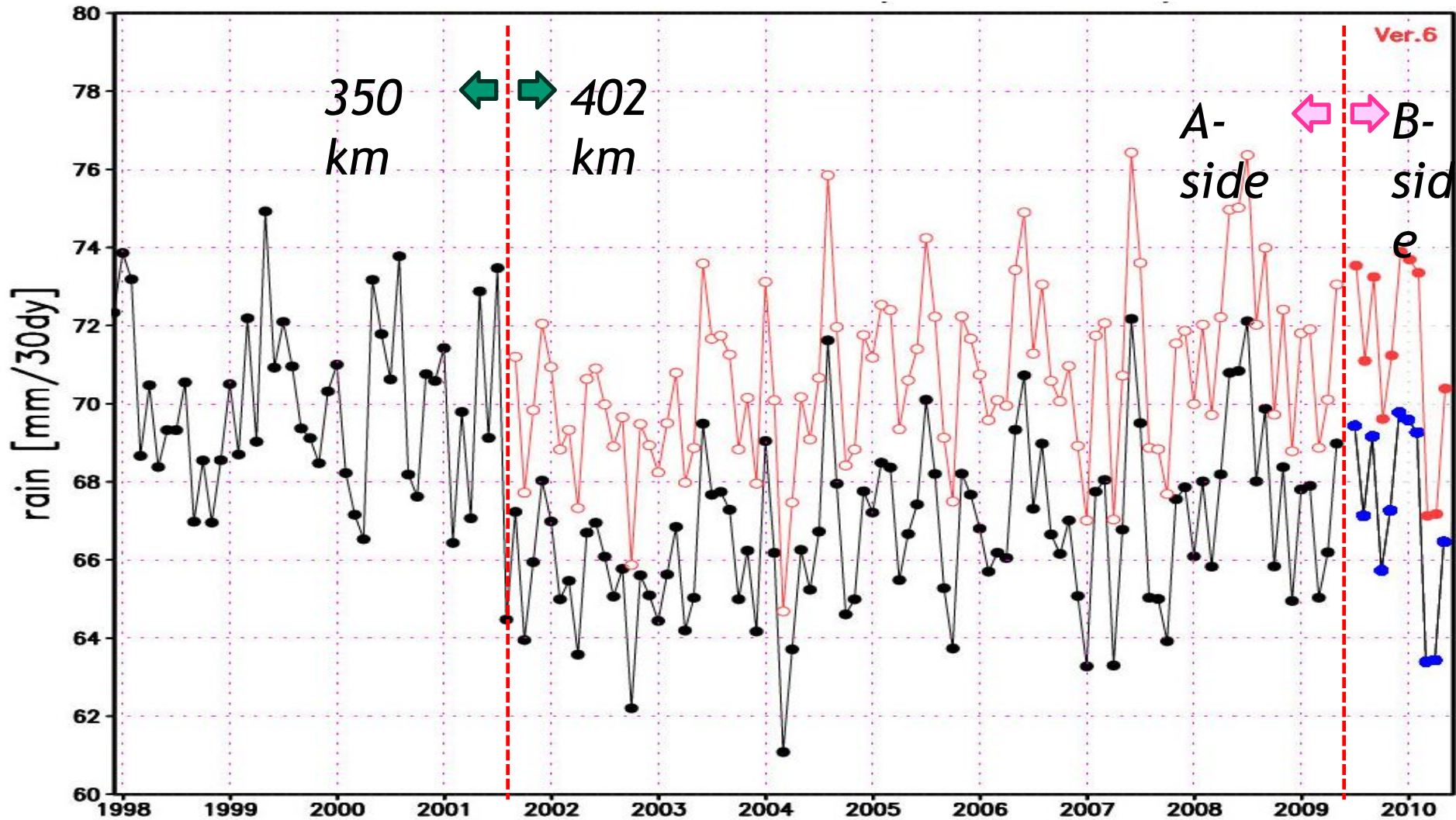
Launched in Nov., 1997. Still under operation

First space-borne precipitation radar developed by CRL and NASDA

Orbit	Circular (Non-Sun Synchronous)
Altitude	350km (402.5km since Aug. 2001) (± 1.25 km)
Inclination	35 deg.
Sensor	<p>Precipitation Radar (PR)</p> <p>TRMM Microwave Imager (TMI)</p> <p>Visible and Infrared Scanner (VIRS)</p> <p>Clouds and the Earth's Radiation Energy System (CERES)</p> <p>Lightning (LIS)</p>



Global Monthly Accumulated Rain by TRMM/PR (Estimated Surface Rain 1997/12 – 2010/05)



* The total decrease in PR e_{surface} rain by altitude change is estimated to be **5.90%** on average in a global scale.

* Data continuity was kept by calibration for B-side H/W.

Zonal Mean Precipitation

1979–2001 Climatology

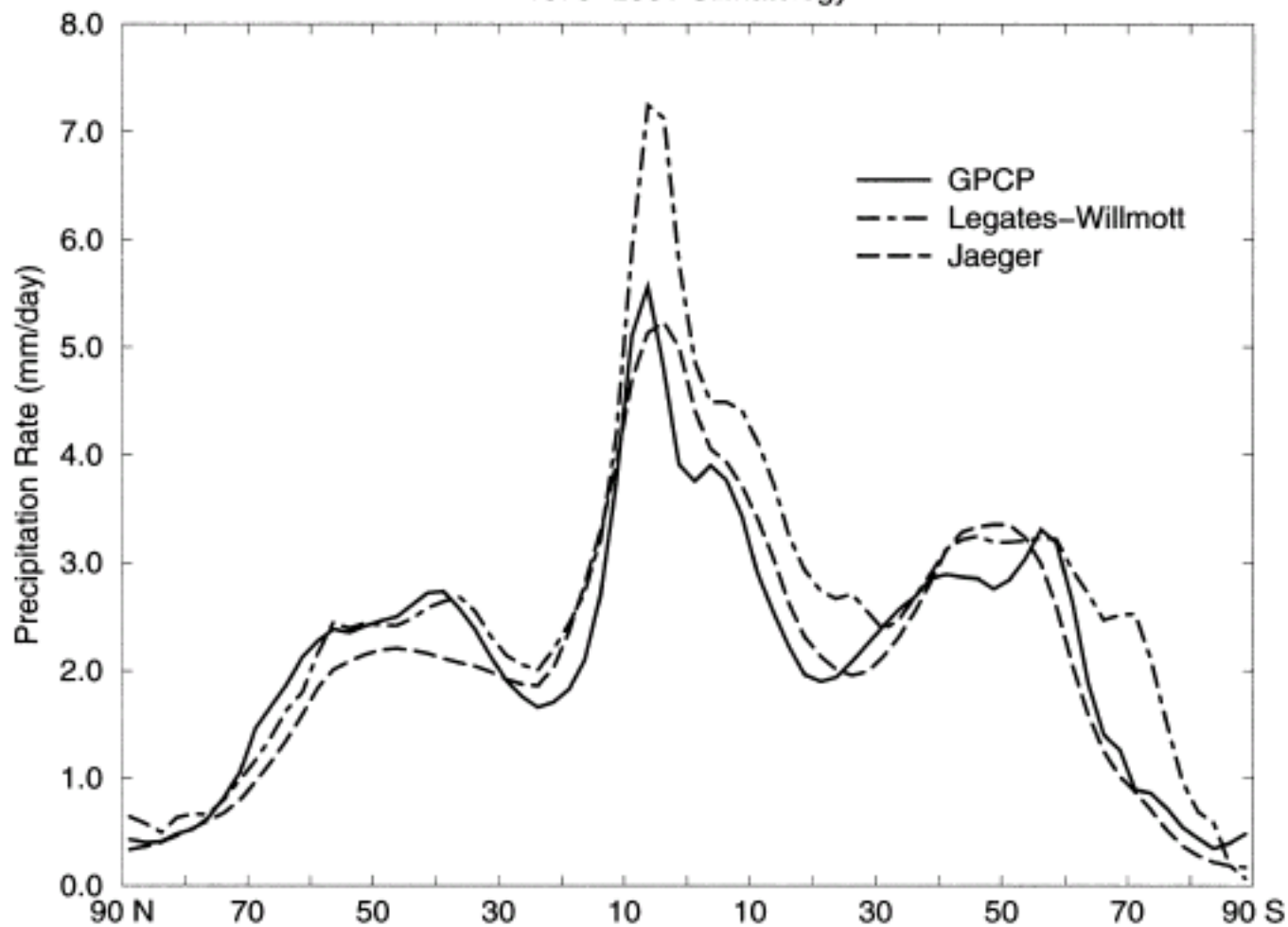


FIG. 5. Zonally averaged annual mean climatologies of precipitation (mm day^{-1}): the GPCP (solid line, see Fig. 4), Legates and Willmott (1990) (dot-dashed line), and Jaeger (1976) (long-dashed line).